ELSEVIER

Catalysis Today 85 (2003) 39–48

CATALYSIS TODAY

www.elsevier.com/locate/cattod

Preparation and characterization of supported $H_3PW_{12}O_{40}$ on silica gel: a potential catalyst for green chemistry processes

José A. Dias*, Ednéia Caliman, Sílvia C.L. Dias, Mônica Paulo, Antonio Thyrso C.P. de Souza

Laboratório de Materiais e Combustíveis, Instituto de Química, Universidade de Brasília, Caixa Postal 04478, Brasília-DF 70919-970, Brazil

Abstract

The solid acidity of 12-tungstophosphoric acid (H_3PW) supported on silica gel has been measured by calorimetry and adsorption in liquid-phase using pyridine as probe. The results indicate a strong interaction of H_3PW with silica, forming a weaker catalyst ($\Delta H_1 = -27.9\,\text{kcal mol}^{-1}$ compared to $\Delta H_1 = -32.7\,\text{kcal mol}^{-1}$ for pure H_3PW). However, there is an increased amount of total titrated protons (sites) for the supported acid, which shows good dispersion of H_3PW over silica. The original low surface area of H_3PW, which implies a small amount of protons available on the surface, is improved by supporting on silica, and their protons become considerably exposed over SiO_2 surface. The dispersion of H_3PW on silica was estimated from XRD pattern, and it decreases with acid content. FTIR spectra of supported H_3PW–SiO_2 reacted with pyridine have shown the characteristic bands of Brönsted acid-type for the strongest site, and a weaker hydrogen-bonded acid-type. FTIR spectra of mechanical mixtures of H_3PW are similar to the supported samples, thus this method cannot distinguish these materials. XRD characteristics can promptly differentiate between supported H_3PW on silica and mechanical mixtures.

Keywords: 12-Tungstophosphoric acid; FTIR spectra; XRD

1. Introduction

Keggin-type heteropolyacids (HPAs) have been extensively studied because they possess many applications relating to strong acidic and redox properties [1–8]. A wide range of acid strength, and relatively high thermal stability of HPAs allows them to be used in several acid-catalyzed reactions in homogeneous solution, liquid–solid and gas–solid heterogeneous reactions. It has been demonstrated that HPAs are much more effective in acid catalysis than protonic mineral and organic such as sulfuric and *p*-toluenesulphonic acids [6]. 12-Tungstophosphoric acid (H_3PW) is considered the strongest heteropolyacid in the series.

Heteropolyacids have been pointed out lately as versatile green catalysts for a variety of reactions (e.g. alkylation and acylation of aromatics, esterification, liquid bi-phase processes) [9,10]. The green aspects of HPAs catalysts have been discussed in terms of fundamental properties of these compounds in order to develop a sustainable chemistry point of view [11]. Use of liquid catalysts such as H_2SO_4, HF, and *p*-toluenesulphonic acid has been traditional, but these are corrosive, toxic, and difficult to separate from reaction solution [12]. There is an interest to substitute those liquid acids by more environmentally friendly solid acids [13]. Among many possible forms

* Corresponding author. Tel.: +55-61-307-2162; fax: +55-61-368-6901.
E-mail address: jdias@unb.br (J.A. Dias).

0920-5861/$ – see front matter © 2003 Elsevier B.V. All rights reserved.
doi:10.1016/S0920-5861(03)00192-5

of HPAs used as catalysts, there are salt derivatives, and supported heteropolyanions.

HPAs have been supported on different solids to increase the surface area. One goal is finding a better catalyst for reactions of non-polar molecules with heteropoly compounds. The nature of reactants determines whether the reaction takes place in the bulk or on the surface of the catalyst [14], and therefore which is the best characteristic for the solid. It is known that HPAs can absorb polar molecules into their bulk leading to a pseudoliquid-phase type of catalysis. Non-polar molecules react only on the surface or between surface layers of the crystal [7]. Because the surface areas of HPAs are usually very low, increasing them through supporting HPAs may produce a catalyst with higher activity for reactions involving non-polar substrates.

Silica gel is the most often used carrier for HPAs. SiO_2–H_3PW supported has been characterized by XRD and TPD (temperature programmed desorption) [15], microcalorimetry with ammonia adsorption [16,17], and MAS-NMR [18,19]. It is claimed that no distinct diffraction peaks appear on the XRD spectra of supported samples, but when loading is higher than 20 wt.% a broad peak occurs at $2\theta = 10^\circ$, characteristic of H_3PW [15]. According to TPD of ammonia adsorption [15], the strength of SiO_2–H_3PW supported is independent of amount of the heteropoly-acid, but total acidity increases with H_3PW content. TPD [15] and microcalorimetry [16,17] with NH_3 indicate that H_3PW supported on SiO_2 is weaker than pure acid. The nature of interaction between H_3PW and SiO_2 has been studied by ^1H and ^{31}P MAS-NMR. No difference in the ^1H NMR spectra of SiO_2 and SiO_2–H_3PW supported is observed up to 50 wt.% of H_3PW, except that the Si–OH line intensity drops as loading of H_3PW increases [18]. It was concluded that at concentrations below 50 wt.% of H_3PW over SiO_2 the proton ambient is different from that one in crystalline H_3PW. This is also confirmed by the shift in the ^{31}P NMR spectra for 3–60 wt.% of H_3PW supported on SiO_2 [13,18,19]. The interaction of SiO_2 with H_3PW is attributed to the formation of $(\equiv SiOH_2^+)(H_2PW_{12}O_{40}^-)$ species [19]. At concentrations up to 20 wt.% of H_3PW, highly dispersed anions species interacting with silica surface are predominant, while at higher than 50 wt.% content crystals of free H_3PW are formed on the silica surface [18]. Various forms of the polyanions were observed on silica surface using TEM (transmission electron microscopy), including isolated molecules and clusters of 50–500 Å in size, according to HPA loading [20].

The goal of this work was to characterize the acidity of H_3PW supported on silica gel by calorimetry and adsorption in liquid-phase (Cal-ad). The Cal-ad method determines the number of sites (n_i), equilibrium constants (K_i), and enthalpies (ΔH_i) for different acid sites present on these solids, which is not obtained by powerful thermal methods such as gas-phase microcalorimetry, and TPD. Comparison of the Cal-ad results with those from free H_3PW and silica gel is discussed. Spectral data from XRD and FTIR were used to identify structural features of H_3PW on the supported samples.

2. Experimental

2.1. Materials and preparation of supported H_3PW

Elemental and TG analysis of the H_3PW (purchased from Aldrich, and recrystallised before preparation of solution for impregnation) revealed 16 moles of water per mole of H_3PW. Cyclohexane obtained from Fisher was purified by drying over 4 Å molecular sieves for 24 h, and then distilled over P_2O_5. Pyridine obtained from Fisher was distilled over CaH_2. Dried samples were stored in a container with 4 Å molecular sieves. Silica used as support was Davisil® silica gel grade 62 with particles within 60–200 mesh and surface area of 260 $m^2\,g^{-1}$, obtained from Aldrich.

The supported H_3PW catalysts were prepared by impregnation method. Aqueous solutions of H_3PW in HCl 0.01 mol l^{-1} (to avoid any hydrolysis of H_3PW) were prepared, with concentrations depending upon the loading required to the support (e.g. 20 wt.% H_3PW) using 10 ml of the solution per gram of silica. The support was added to the solution forming a suspension. The suspension was stirred, and evaporated at 80 °C until dryness. Then the solid was ground to fine particles and dried in a reactor under vacuum. All samples of supported H_3PW–Silica were dried at 200 °C for 6 h under vacuum before any measurement. The concentration of H_3PW on catalysts was

measured by UV-Vis spectroscopy on the initial solutions, and confirmed for tungsten content determined by ICP.

2.2. Spectral data

Beckman DU-650 UV-Vis spectrophotometer and quartz cells of 1.0 and 0.1 cm pathlength were employed for the adsorption experiment and measurements of H_3PW spectra, respectively. Infrared spectra were obtained with Bomen MB-100 spectrophotometer (4 cm^{-1} resolution, and 16 scans) in dried KBr (Merck) pellets. The XRD patterns were collected using a Rigaku D/Max-2A/C with Cu Kα radiation at 40 kV and 20 mA. A 2θ range from 2° to 40° was scanned at 2° min^{-1}.

2.3. Calorimetric and adsorption titrations

For dried samples of supported H_3PW on silica, a diluted pyridine solution in cyclohexane is added to a slurry of the solid in anhydrous cyclohexane, and the measurement of heat evolved and the equilibrium amount of base in solution are determined in two independent experiments. The calorimetric data generates an isotherm of total heat evolved versus the total moles of base added. Calorimetry does not account for the amount of base in solution, but the adsorption measurement provides this information producing an isotherm of moles of base adsorbed (per gram of solid) versus moles of base in solution. It is important that the concentrations of base added and the ratio (V/g) between the volume of solution (V) and the mass of solid used (g) be the same in both calorimetric and adsorption experiments to interchange data. Samples of supported H_3PW (1 g) were weighed and transferred to an isothermal calorimetric cell containing a stir bar. For each titration, 100 ml of cyclohexane was added to the cell. A calibrated syringe, filled with a solution of known concentration of pyridine (e.g. 0.1 mol l^{-1}) was inserted into the cell along with a thermistor and a heater coil. All these operations were carried out in an inert atmosphere glove bag. All details of calorimetric setup have been described elsewhere [21]. Each titration was repeated three times.

The adsorption experiments were carried out using 1 g of solid, weighed inside the dry box, and added to a sealed three neck round bottom flask with 100 ml of cyclohexane. The same calibrated syringe from the calorimetric experiment was used for addition of pyridine in this experiment. Then, a 1 ml sample of solution was removed from the flask and placed into a quartz cell of 1 cm pathlength and 1 ml volume. One milliliter of cyclohexane was added back into the flask in order to maintain a constant volume. The absorbance of pyridine was measured at 251 nm to determine its equilibrium concentration in solution using a calibration curve. Since the amount of pyridine added was known, the amount of base adsorbed by the solid was calculated by difference. Each adsorption experiment was repeated three times.

In addition, to make sure there were no diffusion problems for the experiments, time dependent UV adsorption and heat evolved measurements were performed (three time conditions for each experiment). It was observed for standing times above 3 min, there was no variation on the absorbance or the heat measured. Therefore, the experiments were performed in the time scale of 3 min between each addition of pyridine.

2.4. Cal-ad method of calculation

Solving data from calorimetric and adsorption experiments simultaneously is the base of the Cal-ad analysis [21–23]. The model employs multiple-site equilibrium for the different active sites present in a solid acid. A Langmuir-type equation is summed over all sites of the solid, according to Eq. (1):

$$\frac{h}{g} = \sum \left(\frac{n_i K_i [\mathrm{B}]}{(1 + K_i [\mathrm{B}])} \right) \Delta H_i \quad (1)$$

where h is the sum of the heat evolved (cal) from the calorimetric titration; g the mass of solid (g); [B] the concentration of base in solution at equilibrium (mol l^{-1}); n_i the number of each different site (mol g^{-1}); K_i the equilibrium constant for each site (M^{-1}); and ΔH_i is the enthalpy of reaction for each site on the solid (kcal mol^{-1}).

A simplex routine is used to calculate the parameters. As the calorimetric titration does not measure the equilibrium concentration in solution, this information is obtained through a polynomial series, according to

this expression:

$$\left(\frac{V}{g}\right)[\mathrm{T}] = x^n[\mathrm{B}]^n + x^{n-1}[\mathrm{B}]^{n-1} + x^{n-2}[\mathrm{B}]^{n-2} + x^{n-3}[\mathrm{B}]^{n-3} + \cdots \quad (2)$$

where (V/g) is the ratio of volume of solution (l)/mass of solid (g); [T] the total concentration of base added for each addition in the calorimetric experiment (mol l^{-1}); [B] is the equilibrium concentration of base in solution (mol l^{-1}). The polynomial is one degree higher than the number of sites (e.g. for two sites a third degree polynomial is used as shown in Eq. (2)). The x^n terms have the following meaning for a two site adjustment:

$$x^3 = K_1K_2\left(\frac{V}{g}\right);$$

$$x^2 = n_1K_1K_2 + n_2K_1K_2 - \left(\frac{V}{g}\right)K_1K_2[\mathrm{T}] + \left(\frac{V}{g}\right)K_1 + \left(\frac{V}{g}\right)K_2;$$

and

$$x = n_1K_1 + n_2K_2 - \left(\frac{V}{g}\right)K_1[\mathrm{T}] - \left(\frac{V}{g}\right)K_2[\mathrm{T}] + \left(\frac{V}{g}\right).$$

Estimates of n's and K's are obtained from a Langmuir analysis of the adsorption data using Eq. (3):

$$S_\mathrm{T}B = \sum \frac{n_iK_i[\mathrm{B}]}{(1 + K_i[\mathrm{B}])} \quad (3)$$

where $S_\mathrm{T}B$ is the total number of moles of base adsorbed per gram of solid. Cal-ad method has been successfully applied for calculation of K's, n's, and ΔH's for various solid acids, such as silica gel [21], ZSM-5 [24], TS-1 [25], sulfated zirconia [26], $H_3PW_{12}O_{40}$ [27] and other solid acids.

3. Results and discussion

3.1. FTIR and XRD spectroscopic analysis

The supported H_3PW samples were analyzed by FTIR in order to confirm the presence of the Keggin anion on SiO_2. The $PW_{12}O_{40}{}^{3-}$ Keggin ion structure is well known, and consists of a PO_4 tetrahedron surround by four W_3O_{13} groups formed by edge-sharing octahedra. These groups, are connected each other by corner-sharing oxygens [8]. This structure gives rise to four types of oxygens, being responsible for the fingerprint bands of the Keggin ion between 1200 and 700 cm^{-1}.

Fig. 1 shows the typical bands for absorptions of P–O (1080 cm^{-1}), W = O_t (983 cm^{-1}), W–O_c–W (898 cm^{-1}), and W–O_e–W (797 cm^{-1}). These bands are preserved on the supported samples, but they are broadened and partly obscured because of the strong absorptions of silica gel (~1100, and 800 cm^{-1}). The Keggin bands are more evident for samples with W contents above 8 wt.%. On the other hand, FTIR spectra of mechanical mixtures of H_3PW and SiO_2 on the same concentration range have shown similar characteristics, as pointed out before for silica-supported polyoxomolybdates [28]. Thus, ordinary FTIR cannot distinguish unequivocally the difference between supported H_3PW and mechanical mixtures with silica.

XRD patterns were obtained in order to be sure H_3PW was effectively supported on silica gel, and to evaluate the dispersion state of the acid on support. Fig. 2 shows the powder diffraction of the catalysts. Amorphous silica gel displays only a broad band centered at $2\theta = 22^\circ$. It may be noted some of the diffraction peaks characteristic of crystalline H_3PW appeared on the supported catalysts. The number of matching peaks in the range $2\theta = 10$–50° increases with the heteropolyacid content on the silica support. However, even for the sample with 7.6 wt.% H_3PW, XRD has shown larger peaks at $2\theta = 25.2^\circ$ and 34.4° (typical of pure H_3PW). The peaks become not only more evident on intensity, but also less broad (in comparison with solid state H_3PW pattern) as the concentration of H_3PW increases. Contrasting with supported H_3PW on silica, mechanical mixtures of the acid with SiO_2 exhibit sharp and narrower diffraction lines, as formerly observed [15], more similar to crystalline H_3PW. To make this comparison more effective, XRD of the 25 wt.% H_3PW–SiO_2 supported and a mechanical mixture with identical mass of acid was obtained. The mechanical mixture was prepared by mixing H_3PW with SiO_2, grinding to finer particles, and heating at 200 °C for 4 h. The results displayed on Fig. 3 show clearly the pattern produced by that

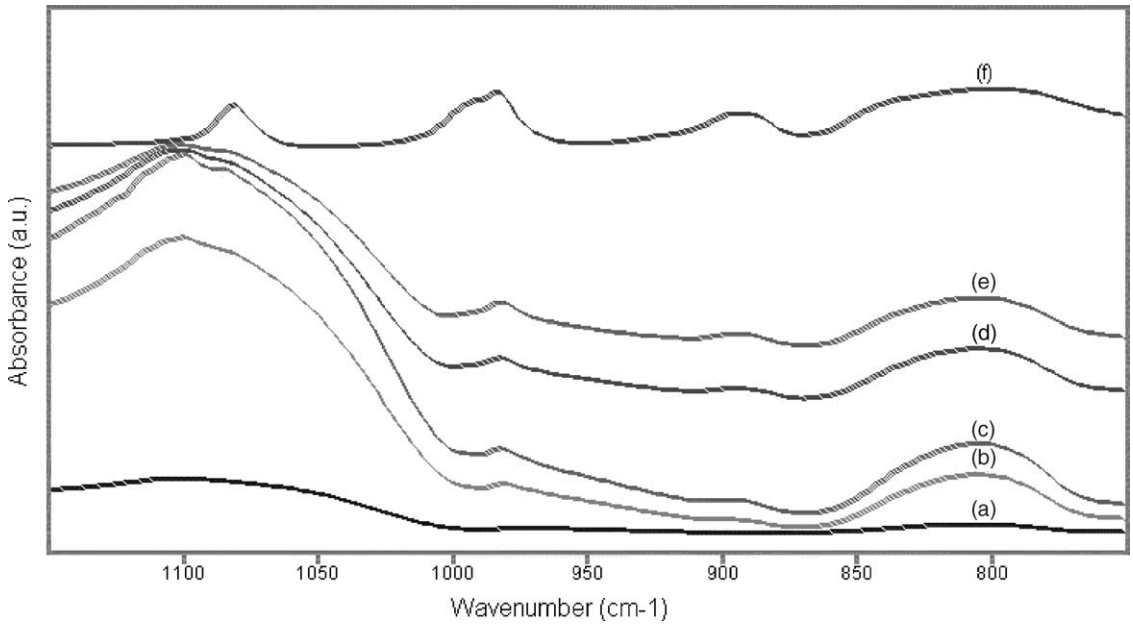

Fig. 1. FTIR spectra of: (a) SiO_2; (b) 7.6 wt.% H_3PW–SiO_2; (c) 15.3 wt.% H_3PW–SiO_2; (d) 19.5 wt.% H_3PW–SiO_2; (e) 24.5 wt.% H_3PW–SiO_2; (f) H_3PW.

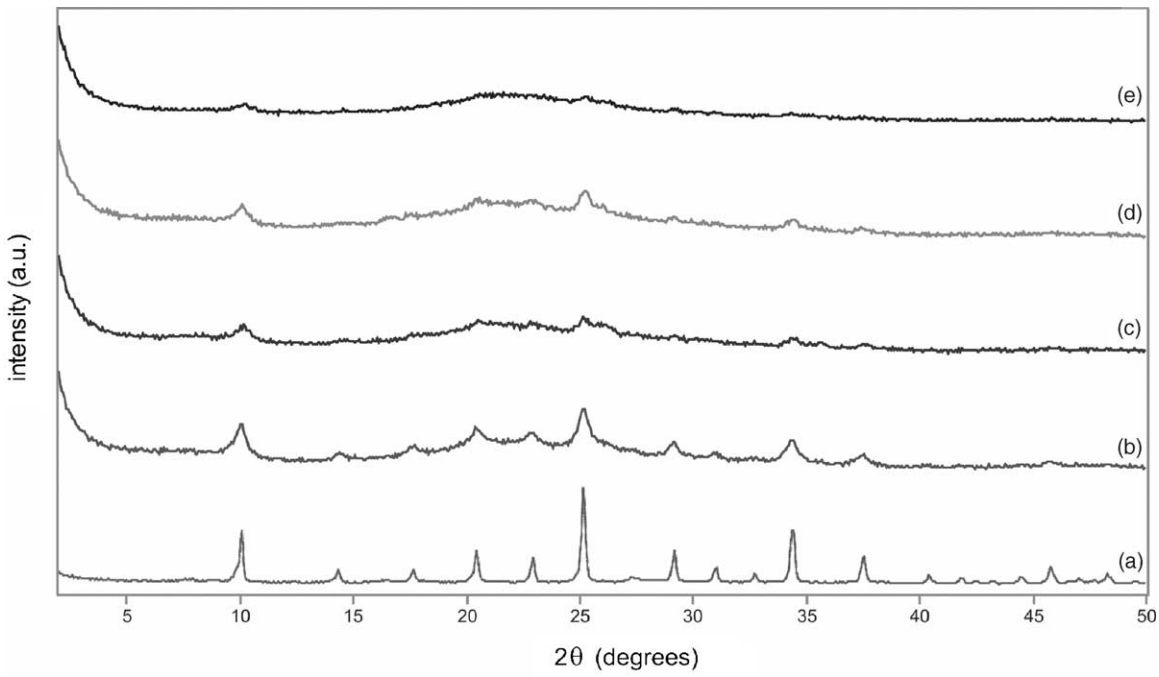

Fig. 2. XRD patterns of: (a) H_3PW; (b) 24.5 wt.% H_3PW–SiO_2; (c) 19.5 wt.% H_3PW–SiO_2; (d) 15.3 wt.% H_3PW–SiO_2; (e) 7.6 wt.% H_3PW–SiO_2.

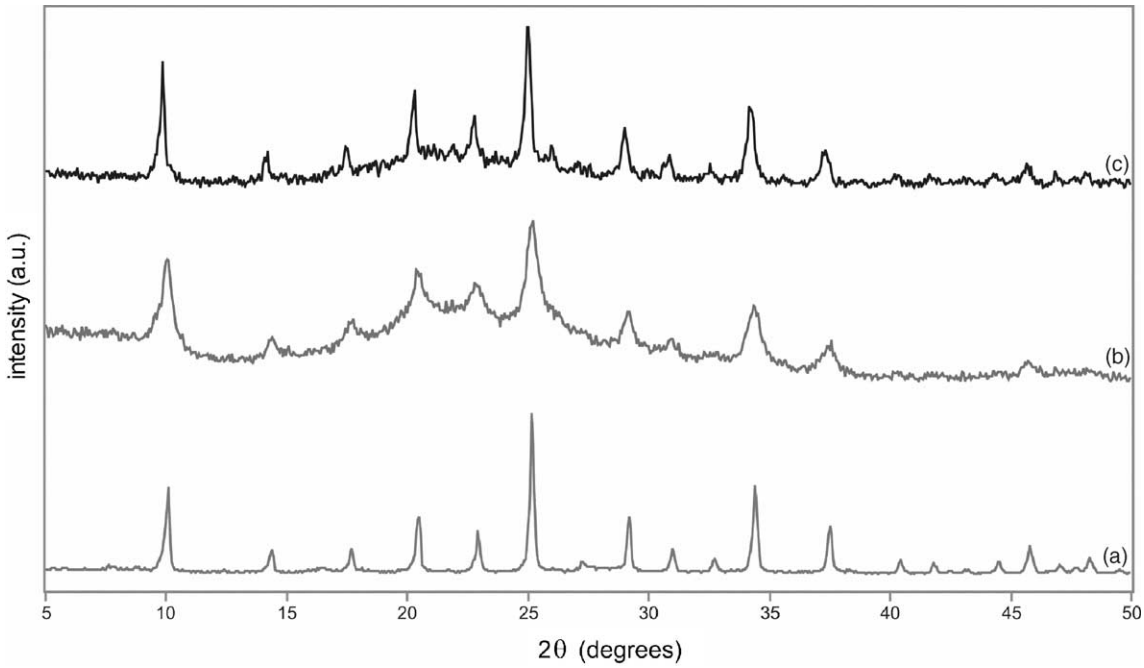

Fig. 3. XRD patterns of: (a) H_3PW; (b) 24.5 wt.% H_3PW–SiO_2 supported; (c) 24.5 wt.% $H_3PW + SiO_2$ mechanical mixture.

mixture resembles the crystalline H_3PW. The characteristic reflections of H_3PW present higher intensities, and are less broad than the supported sample. Indeed, all of these reflections shift to lower angles as consequence of lack of chemical interaction between the solids. It can be concluded that XRD for supported H_3PW is distinctive of mechanical mixtures of these solids, and can be used to characterize these catalysts.

The dispersion of H_3PW on silica gel support has been estimated by the mean crystallite size from the XRD patterns of the catalysts. The equation developed by Scherrer [29] was applied to each sample using $2\theta = 10.2^\circ$ (*h k l* plane (1 1 0)), which is less influenced by the diffracted broad band of non-crystalline silica. The mean diameters of the H_3PW crystallites were 118, 144, 150, and 188 Å for the supported H_3PW–SiO_2 with ca. 8, 15, 20, and 25 wt.% acid loading, respectively. These data indicate a decrease of H_3PW dispersion when increasing acid loading, which is expected based on formation of larger agglomerates on silica surface with concentration of acid impregnated on the support. For comparison, crystalline H_3PW (recrystallized and ground to particles approximately same average size of the supported catalysts) shows a diameter of 320 Å, using the same Scherrer equation. Therefore, higher dispersion of H_3PW clusters is achieved on supported catalysts. The size of crystallites is in the range of that obtained by TEM (50–500 Å) for isolated or agglomerated particle [20].

3.2. Cal-ad analysis of silica-supported H_3PW

Calorimetric titrations with pyridine were performed in supported H_3PW on silica with different loadings of the polyacid. H_3PW loadings ranging from ~8–25 wt.% were studied. Average enthalpies results (calculated based on limiting reagent assumption) for reaction of these solids are presented in Table 1. These semi-quantitative results show that the interaction of H_3PW with SiO_2 is strong ($\Delta H_{AVG} = -26\,kcal\,mol^{-1}$), comparatively to pure SiO_2 [21] ($\Delta H_1 = -12.6\,kcal\,mol^{-1}$) for the strongest site, and almost independent of heteropolyacid content from 15 to 24 wt.% of H_3PW. Loading about 8 wt.% of H_3PW gives lower heats ($\Delta H_{AVG} = -21\,kcal\,mol^{-1}$), probably because at low H_3PW content stronger interaction with silica occurs and the responsible species for

Table 1
Results of calorimetric titrations (25 ± 1 °C) of supported H_3PW–SiO_2 with pyridine in cyclohexane

Sample	H_3PW (wt.%)	H_3PW/g of solid[a] (mmol)	H^+/g of solid[a] (mmol)	$-\Delta H_{AVG}$ (kcal mol^{-1})[b]
HPW25	24.5	0.084	0.252	27
HPW20	19.5	0.068	0.204	26
HPW15	15.3	0.053	0.159	24
HPW8	7.6	0.026	0.078	21

[a] Value based on the real amount of H_3PW supported.
[b] The average enthalpy is based on the first two or three additions of pyridine in the titration, using the limiting reagent approximation. To convert the enthalpy values to kJ mol^{-1} multiply by 4.184.

acidity are different from that at higher content. ^1H and ^{31}P NMR [15,16] confirmed the formation of a strong interaction between H_3PW and SiO_2, and at concentrations up to 20 wt.% the species on the surface are considered isolated. The average enthalpies obtained in this work for these catalysts confirm the spectroscopic results, since interaction is stronger for supports with low content of H_3PW, and less intense with contents above 20 wt.%. Thus, at least partial reaction occurs between H_3PW and SiO_2, forming a weaker acid than the free H_3PW. Finally, these experiments accomplished the objective to obtain a rough estimate of acid strength of those solid acids.

Dispersion of H_3PW over silica on the supported samples is also an important property for this type of catalyst. In this sense, the monolayer capacity can be estimated from surface area of silica and relative size of H_3PW crystals. Considering silica gel with 260 m^2 g^{-1} and the Keggin anion occupying about 1.1 nm^2, theoretically loading 52 wt.% of H_3PW saturates the surface. Nonetheless, results of ^{31}P MAS-NMR [13] have indicated that the true saturation of silica surface occurs at much lower acid loading (about 20 wt.% H_3PW). In addition, many works in the literature have used silica as support with acid loading about 20–25 wt.% for different reactions (e.g. [15,17]). Based upon these results, a complete Cal-ad analysis was made on 25 wt.% H_3PW supported on SiO_2.

The calorimetric and adsorption isotherms of 25 wt.% H_3PW–SiO_2 sample reacting with pyridine in cyclohexane are shown in Fig. 4. The Cal-ad data were analyzed assuming the presence of two sites and three sites. Three site fit shows a meaningless

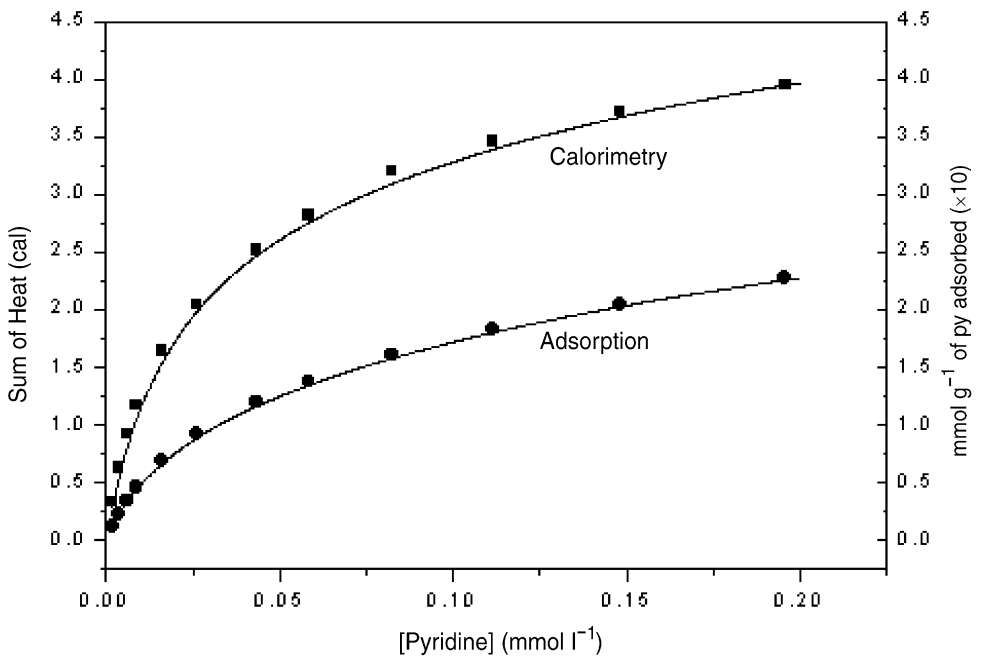

Fig. 4. Isotherms of calorimetry and adsorption of supported 24.5 wt.% H_3PW–SiO_2 reacted with pyridine in cyclohexane.

Table 2
Cal-ad results for supported 24.5 wt.% H_3PW–SiO_2[a] for reaction with pyridine in cyclohexane

n_1 (mmol g^{-1})	0.102 ± 0.005
K_1 (M^{-1})	6.7 ± 0.1 × 10^5
$-\Delta H_1$ (kcal mol^{-1})[b]	27.9 ± 0.7
$-\Delta G_1$ (kcal mol^{-1})	7.9
ΔS_1 (cal $degree^{-1}$)	66.7
n_2 (mmol g^{-1})	0.310 ± 0.061
K_2 (M^{-1})	3.8 ± 0.7 × 10^4
$-\Delta H_2$ (kcal mol−1)[b]	10.1 ± 2.9
$-\Delta G_2$ (kcal mol^{-1})	6.2
ΔS_2 (cal $degree^{-1}$)	12.8

[a] Davisil® silica gel grade 62 with surface area of 260 m^2 g^{-1}.
[b] To convert the enthalpy values to kJ mol^{-1} multiply by 4.184.

result for the third site with high standard deviation errors for the parameters. The math adjust for two sites gives not only better standard deviations on the parameters, but also has the residual sum of squares in the same order of magnitude of the experimental error of calorimetric apparatus [30]. Table 2 reports the thermodynamic parameters for the interaction of pyridine with supported H_3PW (25 wt.%) calculated by Cal-ad.

The enthalpy for interaction with pyridine of 25 wt.% H_3PW–SiO_2 on the strongest site ($\Delta H_1 = -27.9$ kcal mol^{-1}) is smaller than the enthalpy of pure H_3PW ($\Delta H_1 = -32.7$ kcal mol^{-1}) [27], but the number of sites is higher ($n_1 = 0.102$ mmol g^{-1}) for the supported H_3PW than the free acid ($n_1 = 0.079$ mmol g^{-1}). The second site shows an enthalpy of -10.1 kcal mol^{-1} and a number of sites of 0.31 mmol g^{-1}, while free H_3PW shows $\Delta H_2 = -19.6$ kcal mol^{-1} with $n_2 = 0.16$ mmol g^{-1}. The FTIR spectrum shows the Keggin structure is maintained when H_3PW is supported on silica, but the protons are also connected to silanol groups of silica gel. Therefore, more energy is needed to pyridine displace the proton from the catalyst forming an ion pair, leading to lower interaction enthalpies of this base with supported H_3PW. Nevertheless, on the supported 25 wt.% H_3PW, the total available protons are 0.225 mmol g^{-1} of catalyst (about one-fifth of pure H_3PW). Accordingly, about 45% have the highest strength, while on crystalline H_3PW (total of 1.03 mmol g^{-1} of solid) only 8% of protons correspond to the strongest site. These results suggest that H_3PW is well dispersed on silica gel leading to more protons available on the surface area of catalyst with relatively high acidity. For silica gel treated at 200 °C under vacuum, the thermodynamic parameters obtained [21] were $\Delta H_1 = -5.5$ kcal mol^{-1}, $n_1 = 1.12$ mmol g^{-1}, $\Delta H_2 = -3.2$ kcal mol^{-1}, and $n_2 = 1.30$ mmol g^{-1}. Based on the Cal-ad results, there would be two possibilities to explain the lower heat obtained for the second site of H_3PW–SiO_2 supported. Either the remaining protons of this solid is inaccessible to pyridine molecules, and this leads the titration to neutralize only remaining sites of pure silica gel, or the second site is an average of the weaker sites produced by interaction of remaining protons of H_3PW with silica, and sites of pure silica gel. The total number of sites titrated ($n_1 + n_2 = 0.412$ mmol g^{-1} of solid) indicates not only the protons brought in by H_3PW are neutralized, but there must be a contribution of silica gel in the second site. An average of second site of pure H_3PW ($\Delta H_2 = -19.6$ kcal mol^{-1}) with the two sites of pure silica gel ($\Delta H_1 = -5.5$ kcal mol^{-1} and, $\Delta H_2 = -3.2$ kcal mol^{-1}) would give a site with about $\Delta H \sim -9.4$ kcal mol^{-1}, which is close to the value obtained by the H_3PW–SiO_2 supported ($\Delta H_2 = -10.1$ kcal mol^{-1}). In order to have some evidence for the contribution of sites from silica gel to this Cal-ad result, FTIR spectrum of the supported sample was obtained after reaction with pyridine (Fig. 5). The spectrum shows contribution of pyridine adducts in the region 1800–1400 cm^{-1}. Expanding this region, it can be seen the formation of pyridinium ion by absorptions at 1540, and 1488 cm^{-1}. A band occurring at 1640 cm^{-1} is not conclusive (although considered as pyridinium ion) because some water was presented on the preparation of the pellet sample. Also, there is a small band at 1447 cm^{-1} due to hydrogen-bonded pyridine [31], which is present on pure silica gel after reaction with pyridine [21]. Thus, it can be concluded the first site of 25 wt.% H_3PW–SiO_2 supported is Brönsted-type, and the second one is hydrogen-bonded type, which accounts for the magnitude orders of enthalpies (ΔH_1 and ΔH_2) obtained by Cal-ad. This FTIR spectrum clearly shows some contribution of silica gel surface sites on the supported samples, since only pyridinium ion is present on pure H_3PW [27]. Therefore, the second site of H_3PW–SiO_2 supported is probably an average of the second site of pure H_3PW and silica gel.

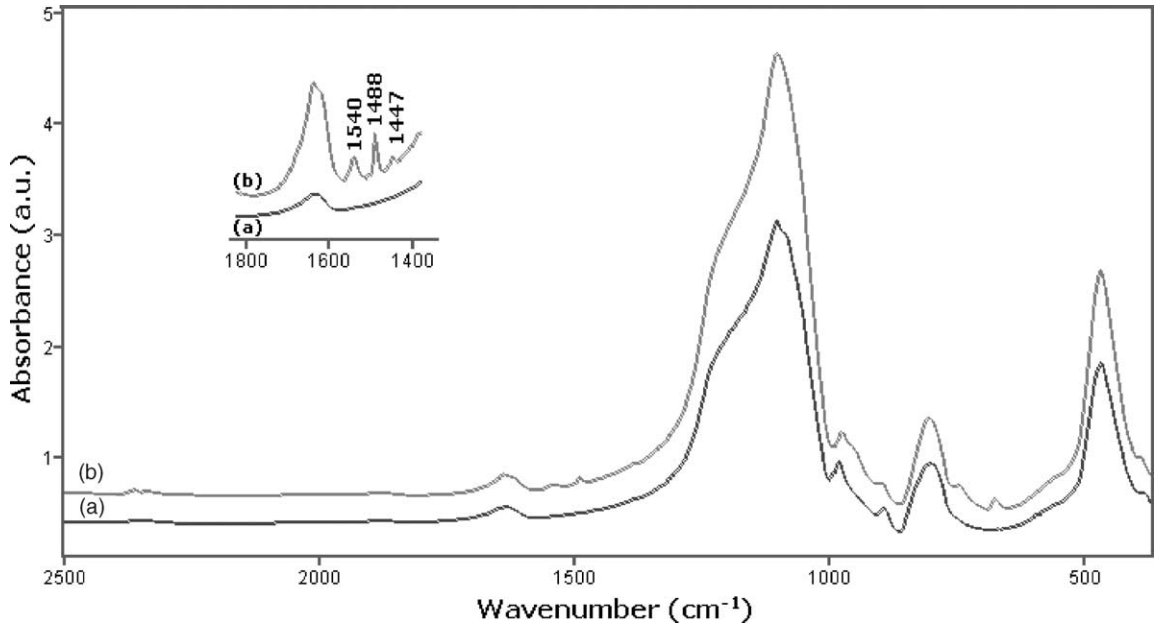

Fig. 5. FTIR spectra of 24.5 wt.% H_3PW–SiO_2 supported: (a) before, and (b) after reaction with 0.412 mmol of pyridine per gram of catalyst.

Comparison of acidity obtained by Cal-ad with other methods is illustrative. The Cal-ad results are not similar from TPD measurements with ammonia [15], since no differences on desorption maximum was evidenced. It should be mentioned that the samples on that report were activated at much higher temperature (500 °C), and TPD profiles of supported samples has shown broad peaks. Thus, the maximum on TPD curves may be not so accurately determined. On the other hand, microcalorimetry of ammonia adsorption measurements [16,17] gave parallel results of Cal-ad, indicating the supported H_3PW on silica gel is a weaker acid than the free acid. For a 20 wt.% H_3PW supported on silica, initial heats of ammonia adsorption is about $-170\,kJ\,mol^{-1}$ (approx. $-40.6\,kcal\,mol^{-1}$). This heat drops to approx. $-100\,kJ\,mol^{-1}$ (approx. $-23.9\,kcal\,mol^{-1}$) around the amount of total neutralization of protons [17]. It has been discussed the differences between measurements in gas- and liquid-phase [30,32,33]. The gas–solid data contain a dispersion component not present in solution, which leads to larger measured enthalpies values. In addition, pyridine and ammonia have size and basicity not similar, and comparison is not straight [27]. The smaller size of NH_3 compared to pyridine makes the former molecule reaching acid positions in the lattice that pyridine may not be able to react with. However, it can be conclude, independent of the measurement method, H_3PW supported on SiO_2 is a weaker acid than pure heteropolytungstic acid.

4. Conclusions

This work reports thermodynamic parameters obtained by calorimetry and adsorption measurements for supported H_3PW on silica reacting with pyridine in cyclohexane slurry. The interaction of H_3PW with silica is almost independent of heteropolyacid content from 15 to 25 wt.%. The strength of 25 wt.% H_3PW–SiO_2 supported ($\Delta H_1 = -27.9\,kcal\,mol^{-1}$) is lower than free acid ($\Delta H_1 = -32.7\,kcal\,mol^{-1}$), but the higher amount of available protons titrated with pyridine (about 45% on supported compared to 8% of free acid) from the strongest site demonstrates a much better exposition of these protons. The higher dispersion of H_3PW is confirmed by size of crystallites supported on silica determined by XRD. In addition, XRD patterns can differentiate supported samples

from mechanical mixtures of H_3PW and SiO_2, which cannot be evidenced by FTIR. The nature of sites obtained by Cal-ad reveled pyridinium ion bands for the strongest site (Brönsted) and hydrogen-bonded pyridine to the weaker site of supported H_3PW after reaction with pyridine. The acidic order is consistent to the literature results where free H_3PW is stronger than supported H_3PW–SiO_2.

Acknowledgements

The authors are grateful to the Department of Chemistry of the University of Florida for use of the calorimeter, and Dr. Russel S. Drago (1928–1997) who initially directed part of this work. We thank Prof. Dr. Edi Mendes Guimarães from Laboratório de Difração de Raios-X (IG/UnB) for XRD measurements. Also, we acknowledge CNPq for a scholarship to pursue a Doctorate level (E.C.), and financial supports given by UnB, Finatec, and Finep/CTPetro.

References

[1] N. Mizuno, M. Misono, Chem. Rev. 98 (1998) 199.
[2] T. Okuhara, N. Mizuno, M. Misono, Adv. Catal. 41 (1996) 113.
[3] A. Corma, Chem. Rev. 95 (1995) 559.
[4] C.L. Hill, C.M. Prosser-McCartha, Coord. Chem. Rev. 146 (1995) 407.
[5] I.V. Kozhevnikov, Catal. Rev. -Sci. Eng. 37 (1995) 311.
[6] Y. Izumi, K. Urabe, M. Onaka, Zeolite, Clay, and Heteropoly Acid in Organic Reactions, VCH, Tokyo, 1992.
[7] M. Misono, Catal. Rev. -Sci. Eng. 29 (1987) 269.
[8] M.T. Pope, Heteropoly and Isopoly Oxometalates, Springer-Verlag, Berlin, 1983.
[9] M. Misono, I. Ono, G. Koyano, A. Aoshima, Pure Appl. Chem. 72 (2000) 1305.
[10] M. Misono, T. Inui, Catal. Today 51 (1999) 369.
[11] M. Misono, C.R. Acad. Sci., Ser. IIc 3 (6) (2000) 471.
[12] X. Chen, Z. Xu, T. Okuhara, Appl. Catal. A 180 (1999) 261.
[13] T. Blasco, A. Corma, A. Martínez, P. Martínez-Escolano, J. Catal 177 (1998) 306.
[14] P.A. Jalil, M.A. Al-Daous, A.A. Al-Arfaj, A.M. Al-Amer, J. Beltramini, A.I. Barri, Appl. Catal. A 207 (2001) 159.
[15] Y. Izumi, R. Hasebe, K. Urabe, J. Catal. 84 (1983) 402.
[16] G.I. Kapustin, T.R. Brueva, A.L. Klyachko, M.N. Timofeeva, S.M. Kulikov, I.V. Kozhevnikov, Kinet. Catal. 31 (1990) 896.
[17] S. Shikata, S. Nakata, T. Okuhara, M. Misono, J. Catal. 166 (1997) 263.
[18] V.M. Mastikhin, S.M. Kulikov, A.V. Nosov, I.V. Kozhevnikov, I.L. Mudrakovsky, M.N. Timofeeva, J. Mol. Catal. 60 (1990) 65.
[19] F.J. Lefebvre, Chem. Soc. Chem. Commun. (1992) 756.
[20] S.M. Kulikov, M.N. Timofeeva, I.V. Kozhevnikov, V.I. Zaikovskii, L.M. Plyasova, L.A. Ovsyannikova, Izv. Akad. Nauk SSSR Ser. (1989) 763.
[21] C.W. Chronister, R.S. Drago, J. Am. Chem. Soc. 115 (1993) 4793.
[22] Y.Y. Lim, R.S. Drago, M.W. Babich, N. Wong, P.E. Doan, J. Am. Chem. Soc. 109 (1987) 169.
[23] R.S. Drago, Applications of Electrostatic-Covalent Models in Chemistry, Surfiside Scientific Publishers, Gainesville, 1994.
[24] R.S. Drago, S.C. Dias, M. Torrealba, L. de Lima, J. Am. Chem. Soc. 119 (1997) 4444.
[25] R.S. Drago, S.C.L. Dias, J.M. McGilvray, A.L.M.L. Mateus, J. Phys. Chem. B 120 (1998) 1508.
[26] R.S. Drago, N.E. Kob, J. Phys. Chem. B 101 (1997) 3360.
[27] J.A. Dias, J.P. Osegovic, R.S. Drago, J. Catal. 183 (1999) 83.
[28] C. Rocchiccioli-Deltcheff, M. Amirouche, M. Fournier, J. Catal. 138 (1992) 445.
[29] H.P. Klug, L.E. Alexander, X-Ray Diffraction Procedures for Polycrystalline and Amorphous Materials, Wiley, New York, 1974.
[30] J.A. Dias, S.C.L. Dias, N.E. Kob, J. Chem. Soc., Dalton Trans. 3 (2001) 228.
[31] E.P. Parry, J. Catal. 2 (1963) 371.
[32] C.E. Webster, J.P. Osegovic, B.J. Scott, S.C. Dias, Microporous Mesoporous. Mater. 31 (1999) 205.
[33] R.S. Drago, J.A. Dias, T.O. Maier, J. Am. Chem. Soc. 119 (1997) 7702.